Screening therapeutic EMT blocking agents in a three-dimensional microenvironment

Published in final edited form as:
Integr Biol (Camb). 2013 February ; 5(2): 381–389. doi:10.1039/c2ib20209c.

Screening therapeutic EMT blocking agents in a three-dimensional microenvironment

Amir R. Aref[1,2], **Ruby Yun-Ju Huang**[3,5], **Wei-miao Yu**[4], **Kian-Ngiap Chua**[3], **Wei Sun**[1], **Ting-Yuan Tu**[1], **Jing Bai**[1], **Wen-Jing Sim**[3], **Ioannis K Zervantonakis**[2], **Jean Paul Thiery**[1,3,4], and **Roger D. Kamm**[1,2]

[1]BioSystems and Micromechanics IRG, S16-07, SMART, Singapore 117543

[2]Department of Biological Engineering, Massachusetts Institute of Technology, 77 Massachusetts Ave, Cambridge, MA, 02139, USA

[3]Cancer Science Institute of Singapore, National University of Singapore, MD6, Medical Drive, Singapore 117456

[4]Institute of Molecular and Cell Biology, Proteos, 61 Biopolis Drive, Singapore 138673

[5]Department of Obstetrics & Gynaecology, National University Hospital of Singapore, 1E Kent Ridge Road, Singapore 119228

Abstract

Epithelial–mesenchymal transition (EMT) plays a critical role in the early stages of dissemination of carcinoma leading to metastatic tumors, which are responsible for over 90% of all cancer-related deaths. Current therapeutic regimens, however, have been ineffective in the cure of metastatic cancer, thus an urgent need exists to revisit existing protocols and to improve the efficacy of newly developed therapeutics. Strategies based on preventing EMT could potentially contribute to improving the outcome of advanced stage cancers. To achieve this goal new assays are needed to identify targeted drugs capable of interfering with EMT or to revert the mesenchymal-like phenotype of carcinoma to an epithelial-like state. Current assays are limited to examining the dispersion of carcinoma cells in isolation in conventional 2-dimensional (2D) microwell systems, an approach that fails to account for the 3-dimensional (3D) environment of the tumor or the essential interactions that occur with other nearby cell types in the tumor microenvironment. Here we present a microfluidic system that integrates tumor cell spheroids in a 3D hydrogel scaffold, in close co-culture with an endothelial monolayer. Drug candidates inhibiting receptor activation or signal transduction pathways implicated in EMT have been tested using dispersion of A549 lung adenocarcinoma cell spheroids as a metric of effectiveness. We demonstrate significant differences in response to drugs between 2D and 3D, and between monoculture and co-culture.

Keywords

Epithelial-mesenchymal transition; microfluidic; three-dimensional cell culture; drug treatment; lung cancer

Introduction

Metastasis, the final stage of tumor progression, is responsible for the deaths of most cancer patients.[1] Yet, there are very few drugs currently available that interfere with the advanced stages of the disease.[2] A majority of cancers are of epithelial origin, and the progression of carcinoma has been hypothesized to involve epithelial-mesenchymal transition (EMT).[3] EMT has also been implicated in the formation of tumor-initiating or cancer stem cells and in drug resistance.[4, 5] These studies prompt the development of new strategies for anti-metastatic drugs based on the concept of inhibiting EMT.[6]

Multiple signaling pathways have been associated with EMT of carcinoma cells including activation of tyrosine kinase surface receptors such as epidermal growth factor receptor (EGFR), transforming growth factor-β receptor 1 (TGF-βR1) and hepatocyte growth factor receptor (HGFR/c-Met). Numerous cytokines, extracellular matrix components and matrix metalloproteases also play a major role in EMT.[7–10] Some of these pathways may act in concert through reciprocal interaction between stromal and carcinoma cells to induce EMT.[11] Carcinoma cells with decreased cell-cell adhesion can delaminate from the primary tumor to invade the adjacent stroma and intravasate into blood and lymph vessels. These phenotypic changes, in part driven by transcriptional controls,[12, 13] can be observed in culture within a reasonably short period of time (2–3 d). *In vitro* assays used to screen for anti-metastatic compounds should replicate the local tumor microenvironment to the extent possible, including a microvasculature, growth factors and ECM, in order to better mimic the mechanisms driving tumor progression. Based on this reasoning, *in vitro* drug screening in a more realistic setting in the presence of other interacting cell populations has the potential to accelerate the search for effective drugs that can inhibit the initiation of EMT, with minimal toxicity to normal cells.[5]

Current *in vitro* models for endothelial-tumor co-culture are achieved through either overlaying an endothelial monolayer on top of matrix containing cancer cells[14, 15] using Transwell™ cell culture devices, or bringing the two types of cells into direct contact to form co-spheroids.[15] The former approach does not allow for real-time monitoring of both cell types and their interactions because the membrane inserts are too distant from a microscope objective[16] and neither method preserves the normal morphological arrangement of the two cell types. The use of co-spheroids measures morphological changes of the multi-cellular structure, which is less quantitative, requires a longer term of culture and precludes the ability to examine each cell type in its individually.

Microfluidic devices have been employed in a number of different cell culture applications, with advantages in creating a precisely controlled geometrical, physical and biochemical microenvironment for cells.[17, 18] More recently, methods have been introduced to incorporate multiple cell types in co-culture, simultaneous cell growth on 2-dimensional (2D) surfaces and in 3-dimensional (3D) scaffolds, and control of a variety of biochemical and biophysical factors while providing the capability for real-time imaging with standard microscopy. These methods have been used to study, for example, cancer-endothelial cell interactions,[19] liver cell growth,[20] biochemical gradient-guided cell growth,[21, 22] and migration,[23] and to simulate certain aspects of organ function.[24] While this technology

shows promise in a variety of settings, it has not yet been used to examine EMT, and requires further development before it can be applied to the quantitative assessment of metastatic potential at the molecular and cellular level.

Here, we demonstrate a tumor microenvironment model based on a microfluidic device[25] (Figs. 1A to 1C) capable of 1) recapitulating the physical and biochemical context that allows for the manifestation of EMT of cancer cells in 3D, in the presence of human endothelial cells; and 2) quantitatively monitoring the EMT inhibitory effect of drugs. Cancer cell spheroids transferred to and grown in this device are induced to disperse in 3D and exhibit mesenchymal morphology in a short timeframe, during co-culture with human umbilical vein endothelial cells (HUVECs) without direct cell-cell contact (Fig. 1D). Drugs that block specific signaling pathways introduced to the HUVEC-lined channel beside the cancer spheroid-seeded collagen gel are shown to behave differentially in 3D than in 2D, and interact strongly with the endothelial monolayer. These effects are shown to have a significant effect on the concentration of drug needed to inhibit EMT.

Results

A549 lung adenocarcinoma cells were chosen for their ability to revert from an intermediate mesenchymal-like phenotype to an epithelial-like phenotype with drugs known to interfere with EMT pathways (data not shown). Their intermediate mesenchymal-like phenotype is likely to result from an activated autocrine loop mediated by EGFR[26] and TGF-βR1.[27, 28] These cells respond to inhibitors of the EGFR signaling pathway including EGFR small molecular weight inhibitors and antibodies to EGFR and to AZD 0530, a potent Src inhibitor (Fig. S1A).[29] A549 cells can also respond to A83-01, an ALK5/TGF-βR1 inhibitor (Fig. S1B).[27] An estimated IC50 for EMT reversal on monolayer culture was found to be 630 nM for AZD 0530 and 2500 nM for A83-01 from analysis of phase contrast images.

A549 cells were then analyzed as spheroids under different experimental conditions to test the role of the 2D and 3D environments. In the first experimental setting (2D culture), A549 spheroids were plated onto the surface of tissue culture dishes. Cells delaminating from spheroids began to spread after 2 h of seeding, suggesting that the adhesive strength to the substrate exceeded cell-cell adhesion. In control experiments, the cells continued to disperse over a 24 h period (Fig. 2A). In contrast, spheroids treated with CI-1033, a clinically relevant EGFR inhibitor, did not migrate from the base of the spheroid in contact with the substrate (Fig. 2B). For Cl-1033, 50% inhibition concentration of cell dispersal was attained at 5.2 μM in the 2D assay (Fig. 2C).

3D culture of A549 spheroids was achieved by suspending spheroids in the gel region of the microfluidic system (Fig. 1) in the absence or presence of an endothelial cell monolayer. A first series of experiments was conducted to determine the potential EMT-inducing activity of the endothelial cell culture medium. Results demonstrated that A549 spheroids do not dissociate within a 36 h period of incubation in the presence of the endothelial cell culture medium alone (Fig. 3A) even though it contains fibroblast growth factor basic (FGF-B), EGF, and recombinant-3 insulin-like growth factor-1 (R3-IGF1) and fetal bovine serum (FBS). Spheroids do dissociate, however, in the presence of endothelial cells within 12 h

(Fig. 3B) whereas dissociation is fully suppressed using the EGFR inhibitor CI-1033 at 300nM concentration (Fig. 3C). Confocal immunofluorescence microscopy demonstrated that the increment of vimentin and loss of E-cadherin from the spheroids after co-culturing with HUVECs for 36 h (Fig. 4).

Drugs interfering with EGFR, IGFR, PDGFR and TGF-βRI/ALK5-dependtent activation as well as others acting upon intracellular kinases such as Src, MEK and AKT were tested at different concentrations in the 3D assay in order to determine concentrations needed to produce full inhibition of dispersion in a 36 h period of incubation (Table 1).

In order to investigate the effects of 2D vs. 3D microenvironments on spheroid dispersion, parallel screening experiments were performed using conventional 2D microwells, and the results, expressed in terms of the corresponding IC50 values, were determined. In every case but one, the IC50 dose was considerably higher even than the dose required for full inhibition in 3D (Table 1).

Normalized cell proliferation (N/N_0) was used to evaluate cell growth and normalized cell dispersion (Δ/Δ_0) was used to evaluate cell migration away from the spheroid in the presence of drugs. Twelve drugs were tested, each for at least two concentrations along with one control (dose = 0; n = 12 devices) (Fig. 5). Time-dependent cell proliferation and dispersion (Figs. 5A and 5C) indicated that the control condition exhibited the strongest cancer cell activity in terms of both proliferation and dispersion. Compared with the control condition, increasing drug dose caused a significant ($p<0.05$) decrease in cell proliferation as well as a reduction in cell dispersion (Figs. 5B and 5D). By plotting normalized proliferation against normalized dispersion of cancer spheroids at 36 h (Fig. 6), we are able to define four quadrants to characterize the dose response for each drug. The upper right quadrant where the control data points fall indicates cases with high rates of proliferation and dispersion. Most drug-treated data lie in the lower left quadrant corresponding to low proliferation and low dispersion activity. Therefore, it appears that for the conditions tested, whenever the drug was effective in reducing cell dispersion, it also inhibited proliferation. At the higher doses, the effects on proliferation were more marked.

Discussion

The primary purpose of this study was to examine the importance of a 3D microenvironment and co-culture with an endothelial monolayer in the screening of potential drug targets to inhibit EMT. Our rationale was that, as in numerous other biological processes, the nature of the local environment and signaling from neighboring cell types would lead to significant differences in how EMT of an epithelial cell line is manifested. Such differences can be quantified by metrics used to assess the effect of drug on cell spreading and proliferation.

EMT provides a basis for understanding the progression of carcinoma towards dedifferentiated and more malignant states. Most current information about cancer invasion, however, is obtained by the study of cells on 2D surfaces. In reality, cells are physically organized in 3D patterns surrounded by ECM and interacting with other cells *in vivo* and the importance of these factors is now becoming widely recognized.[30–33]

As a step toward replicating *in vivo* conditions, we developed and demonstrated a 3D microfluidic assay, and accompanying imaging and analysis, to characterize the statistics of anti-metastatic drug responses. Our data demonstrate both qualitative and quantitative differences between 2D monolayers of A549 cells and experiments with A549 spheroids in 2D and 3D, and further differences depending on whether or not the tumor cells communicate with a nearby endothelial monolayer. In the case of A83-01 (Fig. S1B), for example, a TGF-βR inhibitor, the differences in effective dose between 2D and 3D culture in the microfluidic system and in combination with endothelial cells were considerable, more than three orders of magnitude (5 nM vs. 2.5 μM). Concentrations of the 12 drugs found to be effective in inhibiting EMT all fall in the range of 1μM or less, suggesting that any of these could be potential candidates for therapy.

The 2D dispersion assay differs considerably from the 3D assay in terms of the spheroid response. For example, in the case of CI-1033, an EGFR inhibitor, the IC50 for inhibition of cell dispersion fell by nearly a factor of 10 comparing 2D dispersion (Fig. 2C) to 3D microfluidic co-culture (Fig. 3A). Furthermore, our data in 3D co-culture are in closer agreement with plasma concentrations for CI-1033 reported to be effective in clinical trials (~10^2 nM). [34, 35] Similar results were found with the remaining eleven drugs. Interestingly, when the spheroids are fully suspended in gel, they remain intact without spreading during the entire 36 h observation period, even in the absence of drug and in the presence of endothelial cell growth medium.

It should be noted that cell migration utilizes different mechanisms depending on whether the migration is on a 2D substrate or through a 3D matrix.[36, 37] Spheroid migration on 2D substrates was earlier described as a competition between cell-cell and cell-substrate adhesion forces.[38] Therefore, different substrates and different size spheroids would play a major role in determining the tendency of the spheroid to disperse. In 3D environments, however, the spheroid is encapsulated by matrix, where migration is not only influenced by the balance of forces, but also by the secretion of matrix metalloproteinases (MMP) needed for ECM remodeling. EMT, in part, is known to promote MMP secretion. Indeed, recent study[36] has demonstrated that there is little overlap between the signaling pathways used in 2D and 3D migration. In addition, cell-cell signaling plays a critical role, as demonstrated here between the HUVEC monolayer and the tumor cells, and this signaling also likely to differ between the 2D and 3D conditions. Therefore, our results suggest the importance of more realistic *in vitro* screening methods in identifying drugs that might inhibit cell dispersion *in vivo*. A change in the local environment, whether the cells are embedded in collagen gel or in contact with a rigid surface, can significantly alter the concentration of drug needed to inhibit the EMT response.

Rapid dissociation of the compact A549 spheroids when in communication with the endothelial monolayer can be reversed by inhibitors of EGFR and TGF-βR suggesting that endothelial cells produce EGF[39] and TGF-β[40] family members. It is well-established that A549 can undergo extensive conversion to a mesenchymal-like morphology in response to EGF and with TGF-β,[27, 28] and that antibodies to EGFR can revert A549 cells to an epithelial phenotype. Our collection of data further suggest that several pathways can be activated by endothelial-derived growth factors, and therefore, that drugs could be designed

that inhibit the kinases involved in activation of A549 cells towards metastasis. However, we cannot exclude the possibility that our drug interferes with production or release of EMT-inducing factors by endothelial cells.

Another objective of these studies was to demonstrate the feasibility of using a 3D microfluidic co-culture system as a screening platform for drugs aimed at preventing EMT. The 3D spheroid system in this microfluidic design offers a unique opportunity to screen drugs for their ability to interfere with EMT. The optically transparent microfluidic system not only reproduced the ECM and multi-type cell microenvironment essential for a tumor to develop *in vivo*, but also provided a means for quantitative, automatic detection of cells and measurement of indices reflecting EMT progression in a time-dependent manner.

Modifications to this system could allow for high throughput screening of new compounds or combination therapies that maximize the inhibition of EMT while minimizing other adverse off target effects. Other cell types in addition to endothelial cells could also be added, either in the gel or the HUVEC-lined channel, to create a more realistic testing environment. Variations on the present design could also address other steps in the metastatic cascade such as local invasion and intravasation. Since few methods exist today for screening drugs directed at reversing metastatic potential, systems such as this that mimic aspects of the tumor microenvironment could prove extremely useful.

Materials and Methods

Generation of A549-H2B-mCherry stable cells

The human lung carcinoma cell line A549 was obtained from ATCC (CCL-185) and grown in DMEM supplemented with 10% FBS. The plasmid pH2B_mCherry_IRES_puro2 was obtained from Addgene (Addgene plasmid 21045).[41] A549 cells grown to 50~70% confluency were transfected with FuGENE 6 (Roche). Red fluorescence at the nuclei indicated a positive transfection. After 48 h, transfected A549 cells were treated with puromycin at a concentration of 2.5 μg/ml. Cells surviving puromycin selection were sorted using fluorescence-activated cell sorting FACS-Aria cell sorter (BD Science, USA) to obtain the most brightly fluorescent cells and were subsequently maintained in serial passages under puromycin selection to generate stable H2B-mCherry expressing A549 cells.

Cell maintenance and preparation of tumor spheroids

Human lung adenocarcinoma A549 cells (ATCC, US) stably expressing histone H2B-mCherry were cultured in T75 flasks (Nunclon Δ-Surface, NUNC, Denmark), and passaged once the cells exceeded 80% confluence. Every two days the culture medium was replenished with Dulbecco's modified Eagle medium (Gibco/Invitrogen 12100, USA) supplemented with 10% fetal bovine serum (Gibco/Invitrogen, USA), 1 μg/ml puromycin (Sigma-Aldrich, St. Louis, MO, USA), 100 units/ml penicillin - 100 units/ml streptomycin (1× pen-strep, Invitrogen). Human umbilical vein endothelial cells (HUVEC) (Lonza, Basel, Switzerland) were maintained in microvascular endothelial growth media (Lonza EGM-2MV, Basel, Switzerland), i.e., Endothelial Basal Media - 2 (EBM - 2) supplemented with SingleQuots ® including 5%(25 ml per 500 ml bottle) FBS, 1× pen-strep and

hydrocortisone 0.2 ml, hFGF-B, 0.2 ml; vascular endothelial growth factor (VEGF), 0.5 ml; R3-IGF-1, 0.5 ml; ascorbic acid, 0.5 ml; heparin, 0.5 ml; hEGF, 0.5 ml; and GA-1000, 0.5 ml. Both cell lines were dissociated using 0.05% trypsin–ethylenedinitriletetraacetic acid (trypsin–EDTA) (Sigma-Aldrich, St. Louis, MO, USA) at 37 °C in an incubator for 3 min followed by medium – inhibition of enzymatic reaction and single cells in suspension were counted with a hemocytometer. We have herein prepared two different types of EGM-2MV, one with VEGF and the other without. The one with VEGF was used to maintain the HUVEC culture, while the other one is applied in seeding HUVEC in the devices, to prevent unwanted exogenous VEGF degradation of collagen gel.

To generate spheroids, A549 cells were trypsinized and resuspended as individual cells at 2~4k cells/ml in DMEM,[42] and seeded onto a 100 mm ultra-low attachment dish (Corning Inc, NY, USA). These cells were cultured for 10–14 d and collected upon spheroid formation (visible under microscopy and >40 μm). In our experiments, individual spheroids were sieved via 100 μm and 40 μm cell strainers to yield spheroids 40–70 μm in diameter, and centrifuged to separate them from the supernatant.

Microfluidic Device Design

The microfluidic tissue culture devices used in this study are described in detail by Farahat et al.[25] The devices (Fig. 1) consist of 2 media channels running parallel to and located on either side of an extended central region containing the extracellular gel matrix, all formed by bonding a coverslip to a patterned polydimethylsiloxane (PDMS) substrate. By varying the composition of the growth media in the channels, drugs, growth factors or other agents can be introduced, either at uniform concentration or as a gradient across the gel region, to elicit cellular responses. Spheroid or individual cell behavior can be observed via 3D confocal imaging of the gel region through the supporting glass coverslip.

Device Fabrication and Cell Seeding in 3D Matrix

The devices were fabricated in PDMS (Dow Corning® Sylgard 184) at a ratio of 10:1 polymer to cross-linker using standard soft lithography techniques.[43] Devices were autoclaved in DI water for 20 min followed by a dry autoclave cycle for 20 min and baked overnight at 80°C to dry. Glass cover slips (#1.5 Cell Path, UK) were then plasma bonded to the PDMS substrate that had been pretreated with ethanol and dried. All device channels were then treated with 1 mg/ml poly-D-lysine (PDL) solution (Sigma-Aldrich, USA) for 4 h to enhance cell and collagen matrix binding to PDMS,[33] followed by another round of drying at 80°C for 24–48 h to make the devices hydrophobic.

200 μl collagen gel solution at 2.5 mg/ml and pH 7.4 was prepared on ice with 126.1 μl type I collagen (3.87 mg/ml, BD Biosciences Cat. No. 354236), 20 μl PBS (10x) with phenol red (Gibco/Invitrogen 14080-055, USA), 43.1 μl deionized water, 7 μl NaOH (0.5N), and 20 μl cell suspension medium with 30–50 tumor spheroids.[44] The specific gel composition was decided upon through a set of preliminary experiments in which we sought a balance between rapid matrix degradation by endothelial cells for low collagen concentrations and impaired cancer cell migration at high concentrations. Spheroid-containing collagen gel solution was then pipetted into the central gel region at low pressure to avoid spillage into

the side channels. Gel is confined to the central gel cage by means of surface tension. Once in place, collagen gel solution was kept in a humidity box in at 37°C for 40 min to allow gel polymerization via thermal cross-linking. DMEM and EGM-2MV with HUVECs were subsequently introduced to respective media channels. After 1–2 h, HUVECs attached in endothelial cell growth channel and formed a semi-confluent monolayer on the coverslip bottom substrate and onto the gel surface. The conditioned medium produced by HUVEC secretions diffuses into the adjacent collagen gel. Average distance between the HUVEC and tumor spheroids was ~200 μm, facilitating rapid cell-cell signaling.

Immunofluorescent staining

Cell culture media was removed from the devices and samples in the microfluidic devices were first rinsed in cold PBS and then fixed in 4% PFA (Sigma-Aldrich, St. Louis, MO, USA) for 15 min at room temperature. Then 0.1% Triton-X (Sigma-Aldrich, St. Louis, MO, USA) was added and incubated for 5 min before blocking by Block Ace (Dainippon Phamaceutical, Osaka, Japan) for 2 h. To demonstrate the endothelial cell monolayer formation, staining of VE-cadherin (1:100, mouse; Sigma Aldrich, USA) was carried out. For analysis of epithelial marker expression, E-cadherin (1:100, mouse; Sigma Aldrich, USA) was used to stain for cell-cell junctions; and nuclei were stained with DAPI (Sigma-Aldrich, USA). Fluorescent images were obtained using FluoView 1000 confocal microscopy (Olympus, Japan). The secondary antibody used was 2mg/ml Alexa Fluor 488-conjugated anti-mouse IgG antibodies (Invitrogen, USA). For analysis of vimentin expression, vimentin (1:200, rabbit; Invitrogen, USA) was used and incubated again with 2 mg/ml Alexa Fluor 488-conjugated anti-rabbit IgG antibodies (Invitrogen, USA), and DNA was labeled by Hoechst (Invitrogen, USA). Fluorescent images were obtained using a phase-contrast microscope equipped for fluorescence (Nikon, Japan).

2D Drug Screening

Twelve kinase inhibitors acting on different targets were selected (Table 1), based on a preliminary screen showing their inhibitory potential on A549 EMT reversal in 2D culture at 2.5 μM concentration (Fig. S1). A549 cells were grown in 96-well plates on 2D from a sparse density of 800 cells/cm^2 and cultured in the presence of concentration of 0.04, 0.16, 0.63, 2.5, 10μM. Cells were imaged after 72 h incubation using IX51 with 10x objective (Olympus, Japan).

2D dispersion assay achieved by culturing spheroids in tissue culture dishes was also studied over 24 h (Fig. 2). Spheroids were seeded in a 96-well plate (Falcon, USA) with ~10–20 per well. Spheroids were supplemented with DMEM medium, and for a range of CI-1033 concentrations: 10, 50, 100, 500, 1,000, 5,000, 10,000, 50,000, and 100,000 nM. For the remaining eleven drugs, concentrations of 5, 50, 500, 5,000, and 50,000 nM were used. IC50 of each drugs were summarized (Table 1).

3D Drug Screening

An appropriate range of concentrations to study was identified through an initial series of experiments in the microfluidic device under 3D conditions. Some of these compounds are approved by the U.S. Food and Drug Administration (FDA) or are currently being used in

clinical trials for the treatment of lung cancer (e.g. Gefitinib and AZD 0530). As noted in Table 1, some of these compounds primarily block receptor activation while others act intracellularly to inhibit specific signaling pathways known to be activated during EMT. Drugs were mixed with both cancer and endothelial cell media, and applied in both channels.

Image Acquisition and Analysis

Three dimensional image stacks of each studied spheroid were acquired using FluoView 1000 confocal microscopy (Olympus, Japan) with a 10X objective (NA = 0.4). Three image channels were acquired for each stack: GFP, mCherry, and transmitted light. Each imaging volume encompassed a 1272.32 micron by 1272.32 micron region allowing simultaneous observation of endothelial cell channel and spheroids. The volumetric Z-stack covered a range of ~160 μm over 18–20 slices per stack. Images were acquired at 0, 12 and 36 h.

From the spatial coordinates of the centroids of all nuclei determined through the process of segmentation, de-noising, and edge-enhancement (see Supplemental Information), we first compute the spheroid center, x_s, then the standard deviation of nuclei from the spheroid center,

$$\Delta = \sqrt{\sigma_x^2 + \sigma_y^2 + \sigma_z^2}$$

which is termed the “dispersion” both in 2D dispersion assay and in 3D microfluidic co-culture of a spheroid. Two metrics are used to assess drug efficacy: normalized dispersion, Δ/Δ_0, and normalized cell number (N/N_0) where the normalizing values (Δ_0 and N_0) are the values at t=0.

The “effective dose” in 3D microfluidic co-culture was determined as the lowest tested concentration deemed sufficient to prevent dispersion (Table 1), i.e., the concentration at which Δ/Δ_0 at t=36 h < 1.42. In cases for which IC50 values of 2D dispersion assay are reported, its determination is based on a curve-fit to the data for at least 5 different concentrations of a particular drug with a minimum of 3 repeats for each condition.

Conclusion

EMT provides a new basis for understanding the progression of carcinoma towards dedifferentiated and more malignant states. However, most of the current information about cancer invasion is obtained by the study of tumor cells acting by themselves in a non-physiologic environment on 2D surfaces. In reality, cells are physically organized *in vivo* in 3D patterns surrounded by ECM as well as other cell types. As a step toward a more realistic *in vitro* assay, we developed and demonstrated a 3D microfluidic system, and accompanying image analysis process to characterize the statistics of anti-metastatic drug responses. Results confirm the importance of growing cells in 2D vs. 3D and that other cell types, in this case endothelial cells, can significantly alter the levels of drug required to inhibit EMT. These studies therefore offer a new approach in drug screening with the potential to better

replicate the *in vivo* microenvironment. They also offer the prospect of including other cell types and matrices to produce even greater realism with tissue-specific characteristics in future studies.

Supplementary Material

Refer to Web version on PubMed Central for supplementary material.

Acknowledgments

This research was supported by the National Research Foundation Singapore through the Singapore-MIT Alliance for Research and Technology's <BioSyM IRG> research programme, by the Cancer Science Institute at the National University of Singapore, and by IMCB core funding A*STAR.

References

1. Ali-Fehmi R, Semaan A, Sethi S, Arabi H, Bandyopadhyay S, Hussein YR, Diamond MP, Saed G, Morris RT, Munkarah AR. Cancer. 2011; 117:301–309. [PubMed: 20818651]
2. Altekruse S, Kosary C, Krapcho M, Neyman N, Aminou R, Waldron W, Ruhl J, Howlader N, Tatalovich Z, Cho H, Mariotto A, Eisner M, Lewis D, Cronin K, Chen H, Feuer E, Stinchcomb D, Edwards Be. 2010 posted to the SEER web site.
3. Thiery JP. Nat Rev Cancer. 2002; 2:442–454. [PubMed: 12189386]
4. Gupta PB, Onder TT, Jiang G, Tao K, Kuperwasser C, Weinberg RA, Lander ES. Cell. 2009; 138:645–659. [PubMed: 19682730]
5. Polyak K, Weinberg RA. Nat Rev Cancer. 2009; 9:265–273. [PubMed: 19262571]
6. Chua KN, Poon KL, Lim J, Sim WJ, Huang RY, Thiery JP. Adv Drug Deliv Rev. 2011; 63:558–567. [PubMed: 21335038]
7. Page-McCaw A, Ewald AJ, Werb Z. Nat Rev Mol Cell Biol. 2007; 8:221–233. [PubMed: 17318226]
8. Joyce JA, Pollard JW. Nat Rev Cancer. 2009; 9:239–252. [PubMed: 19279573]
9. Thiery JP, Acloque H, Huang RY, Nieto MA. Cell. 2009; 139:871–890. [PubMed: 19945376]
10. Hanahan D, Weinberg RA. Cell. 2011; 144:646–674. [PubMed: 21376230]
11. Scheel C, Eaton EN, Li SH, Chaffer CL, Reinhardt F, Kah KJ, Bell G, Guo W, Rubin J, Richardson AL, Weinberg RA. Cell. 145:926–940. [PubMed: 21663795]
12. Moreno-Bueno G, Fernandez-Marcos PJ, Collado M, Tendero MJ, Rodriguez-Pinilla SM, Garcia-Cao I, Hardisson D, Diaz-Meco MT, Moscat J, Serrano M, Palacios J. Cancer Res. 2007; 67:1927–1934. [PubMed: 17332319]
13. Peinado H, Rafii S, Lyden D. Cancer Cell. 2008; 14:347–349. [PubMed: 18977322]
14. Kargozaran H, Yuan SY, Breslin JW, Watson KD, Gaudreault N, Breen A, Wu MH. Clin Exp Metastasis. 2007; 24:495–502. [PubMed: 17653824]
15. Ingthorsson S, Sigurdsson V, Fridriksdottir A Jr, Jonasson JG, Kjartansson J, Magnusson MK, Gudjonsson T. BMC Res Notes. 2010; 3:184. [PubMed: 20609224]
16. Yamakawa S, Furuyama Y, Oku N. Biol Pharm Bull. 2000; 23:1264–1266. [PubMed: 11041266]
17. Tourovskaia A, Figueroa-Masot X, Folch A. Lab Chip. 2005; 5:14–19. [PubMed: 15616734]
18. El-Ali J, Sorger PK, Jensen KF. Nature. 2006; 442:403–411. [PubMed: 16871208]
19. Chung S, Sudo R, Mack PJ, Wan CR, Vickerman V, Kamm RD. Lab Chip. 2009; 9:269–275. [PubMed: 19107284]
20. Toh YC, Zhang C, Zhang J, Khong YM, Chang S, Samper VD, van Noort D, Hutmacher DW, Yu H. Lab Chip. 2007; 7:302–309. [PubMed: 17330160]
21. Vickerman V, Blundo J, Chung S, Kamm R. Lab Chip. 2008; 8:1468–1477. [PubMed: 18818801]
22. Kothapalli CR, van Veen E, de Valence S, Chung S, Zervantonakis IK, Gertler FB, Kamm RD. Lab Chip. 2011; 11:497–507. [PubMed: 21107471]

23. Shamloo A, Heilshorn SC. Lab Chip. 2010; 10:3061–3068. [PubMed: 20820484]
24. Sudo R, Chung S, Zervantonakis IK, Vickerman V, Toshimitsu Y, Griffith LG, Kamm RD. FASEB J. 2009; 23:2155–2164. [PubMed: 19246488]
25. Farahat WA, Wood LB, Zervantonakis IK, Schor A, Ong S, Neal D, Kamm RD, Asada HH. PLoS One. 2012; 7:e37333. [PubMed: 22662145]
26. Jaramillo ML, Banville M, Collins C, Paul-Roc B, Bourget L, O'Connor-McCourt M. Cancer Biol Ther. 2008; 7:557–568. [PubMed: 18296914]
27. Kasai H, Allen JT, Mason RM, Kamimura T, Zhang Z. Respir Res. 2005; 6:56. [PubMed: 15946381]
28. Kim JH, Jang YS, Eom KS, Hwang YI, Kang HR, Jang SH, Kim CH, Park YB, Lee MG, Hyun IG, Jung KS, Kim DG. J Korean Med Sci. 2007; 22:898–904. [PubMed: 17982242]
29. Green TP, Fennell M, Whittaker R, Curwen J, Jacobs V, Allen J, Logie A, Hargreaves J, Hickinson DM, Wilkinson RW, Elvin P, Boyer B, Carragher N, Ple PA, Bermingham A, Holdgate GA, Ward WH, Hennequin LF, Davies BR, Costello GF. Mol Oncol. 2009; 3:248–261. [PubMed: 19393585]
30. Castello-Cros R, Khan DR, Simons J, Valianou M, Cukierman E. BMC Cancer. 2009; 9:94. [PubMed: 19323811]
31. Linder S, Wiesner C, Himmel M. Annu Rev Cell Dev Biol. 27:185–211. [PubMed: 21801014]
32. Xu R, Boudreau A, Bissell MJ. Cancer Metastasis Rev. 2009; 28:167–176. [PubMed: 19160017]
33. Chung S, Sudo R, Zervantonakis IK, Rimchala T, Kamm RD. Adv Mater. 2009; 21:4863–4867. [PubMed: 21049511]
34. Calvo E, Tolcher AW, Hammond LA, Patnaik A, de Bono JS, Eiseman IA, Olson SC, Lenehan PF, McCreery H, Lorusso P, Rowinsky EK. Clin Cancer Res. 2004; 10:7112–7120. [PubMed: 15534081]
35. Simon GR, Garrett CR, Olson SC, Langevin M, Eiseman IA, Mahany JJ, Williams CC, Lush R, Daud A, Munster P, Chiappori A, Fishman M, Bepler G, Lenehan PF, Sullivan DM. Clin Cancer Res. 2006; 12:4645–4651. [PubMed: 16899614]
36. Meyer AS, Hughes-Alford SK, Kay JE, Castillo A, Wells A, Gertler FB, Lauffenburger DA. J Cell Biol. 2012; 197:721–729. [PubMed: 22665521]
37. Decaestecker C, Debeir O, Van Ham P, Kiss R. Med Res Rev. 2007; 27:149–176. [PubMed: 16888756]
38. Douezan S, Guevorkian K, Naouar R, Dufour S, Cuvelier D, Brochard-Wyart F. Proceedings of the National Academy of Sciences of the United States of America. 2011; 108:7315–7320. [PubMed: 21504944]
39. Tunica DG, Yin X, Sidibe A, Stegemann C, Nissum M, Zeng L, Brunet M, Mayr M. Proteomics. 2009; 9:4991–4996. [PubMed: 19810032]
40. Hannan RL, Kourembanas S, Flanders KC, Rogelj SJ, Roberts AB, Faller DV, Klagsbrun M. Growth Factors. 1988; 1:7–17. [PubMed: 3272801]
41. Steigemann P, Wurzenberger C, Schmitz MH, Held M, Guizetti J, Maar S, Gerlich DW. Cell. 2009; 136:473–484. [PubMed: 19203582]
42. Dontu G, Abdallah WM, Foley JM, Jackson KW, Clarke MF, Kawamura MJ, Wicha MS. Genes Dev. 2003; 17:1253–1270. [PubMed: 12756227]
43. Xia YN, Whitesides GM. Annual Review of Materials Science. 1998; 28:153–184.
44. Shin Y, Han S, Jeon JS, Yamamoto K, Zervantonakis IK, Sudo R, Kamm RD, Chung S. Nat Protoc. 2012; 7:1247–1259. [PubMed: 22678430]
45. Yu WM, Lee HK, Hariharan S, Sankaran S, Vallotton P, Ahmed S. Advances in Visual Computing, Pt 1, Proceedings. 2009; 5875:531–543.
46. Yu W, Lee HK, Hariharan S, Bu WY, Ahimed S. Cytometry Part A. 2010; 77A:379–386.

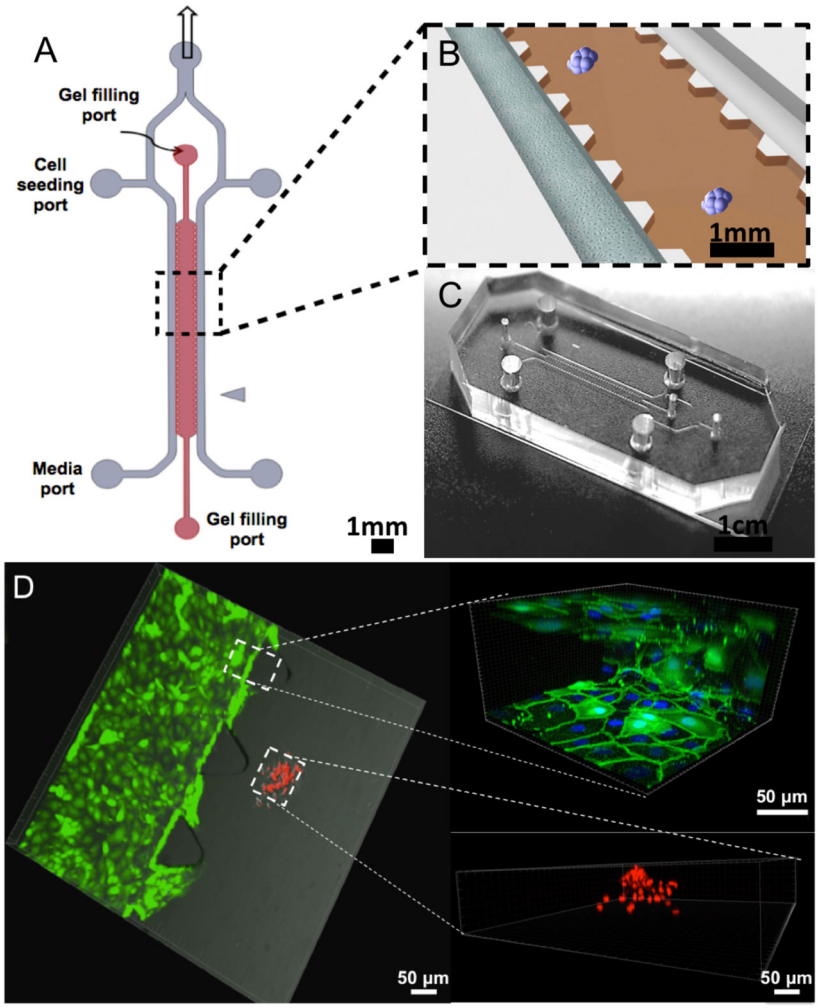

Fig. 1.

Schematic and photograph of 3D co-culture microfluidic device. A. Schematic diagram of device layout depicts the inlets for injecting cells, filling collagen, and replenishing medium. B. Enlarged view of gel region and HUVEC-lined channel. Cytokines in conditioned medium from HUVEC monolayer diffuse into the gel region triggering spheroids to undergo EMT. C. Photograph of the PDMS-molded device bonded on a glass cover-slip. D. A 3D co-culture image combining phase contrast and fluorescence with enlarged HUVECs monolayer structure and 3D cancer spheroid dispersion. Blue: Hoechst; green: VE-Cadherin; red: nuclei mCherry.

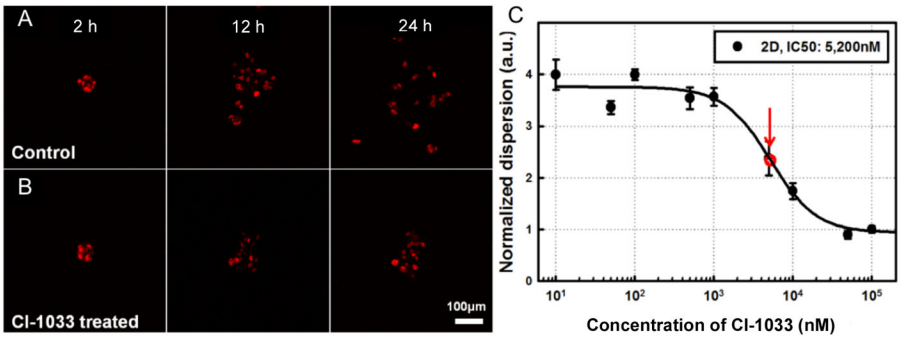

Fig. 2.

Dispersion measurements of A549 spheroids in 2D conditions in a 96-well plate. A. Spheroids were seeded in wells in control medium and allow to spread. B. Treatment with 10 μM CI-1033, an EGFR inhibitor, reduced the dissociation of cancer cells from spheroids. C. 50% inhibition concentration of CI-1033 was achieved at 5,200 nM.

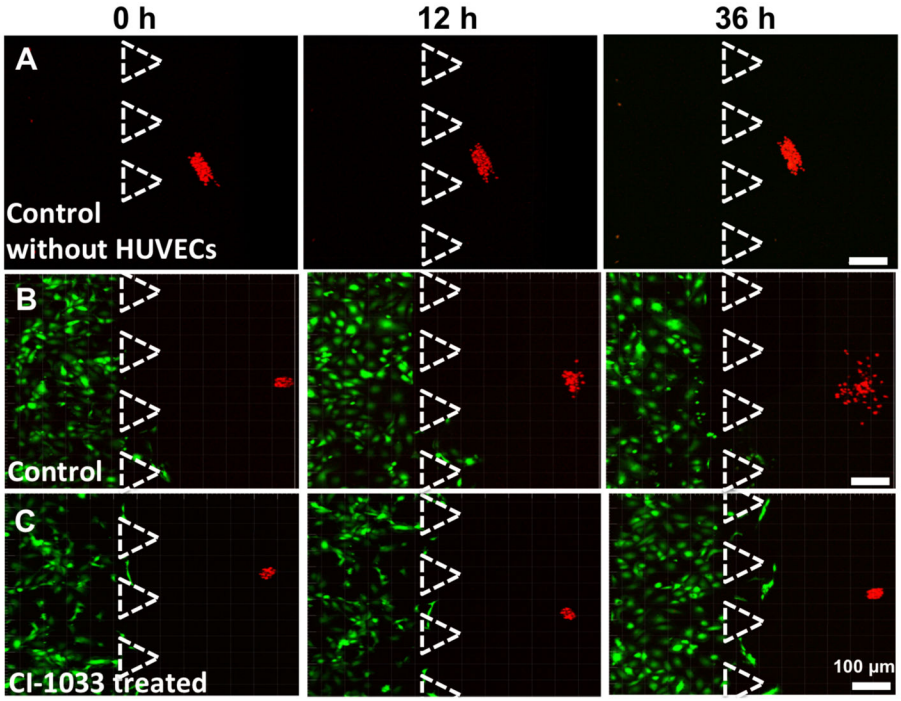

Fig. 3.

Fluorescent images in time-series showing A549 cell dissemination in the 3D collagen gel. A. Control condition in the absence of a HUVEC monolayer, i.e., 3D monoculture. B. Control condition in the presence of a HUVEC monolayer in the side channel, i.e. 3D co-culture. C. EGF-targeted drug (300nM of CI-1033) applied in the presence of HUVEC monolayer. Red: nuclei of A549 cells; green: HUVEC. Triangles show the PDMS posts on the edge of collagen gel.

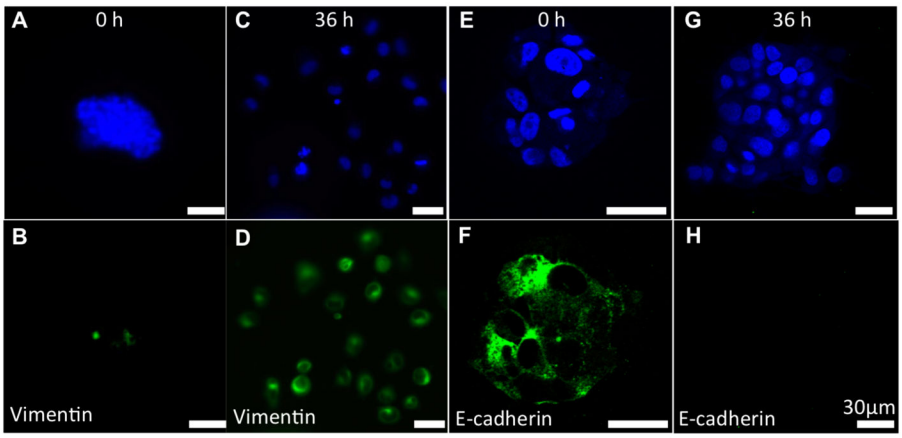

Fig. 4.

Immunostaining of EMT markers on A549 spheroids at 0 h and 36 h in co-culture with HUVECs. A–D. Expression of vimentin in spheroids at 0 h and 36 h. Blue: nuclei; green: vimentin. E–H. Expression of E-cadherin in spheroids at 0 h and 36 h. Blue: nuclei; green: E-cadherin.

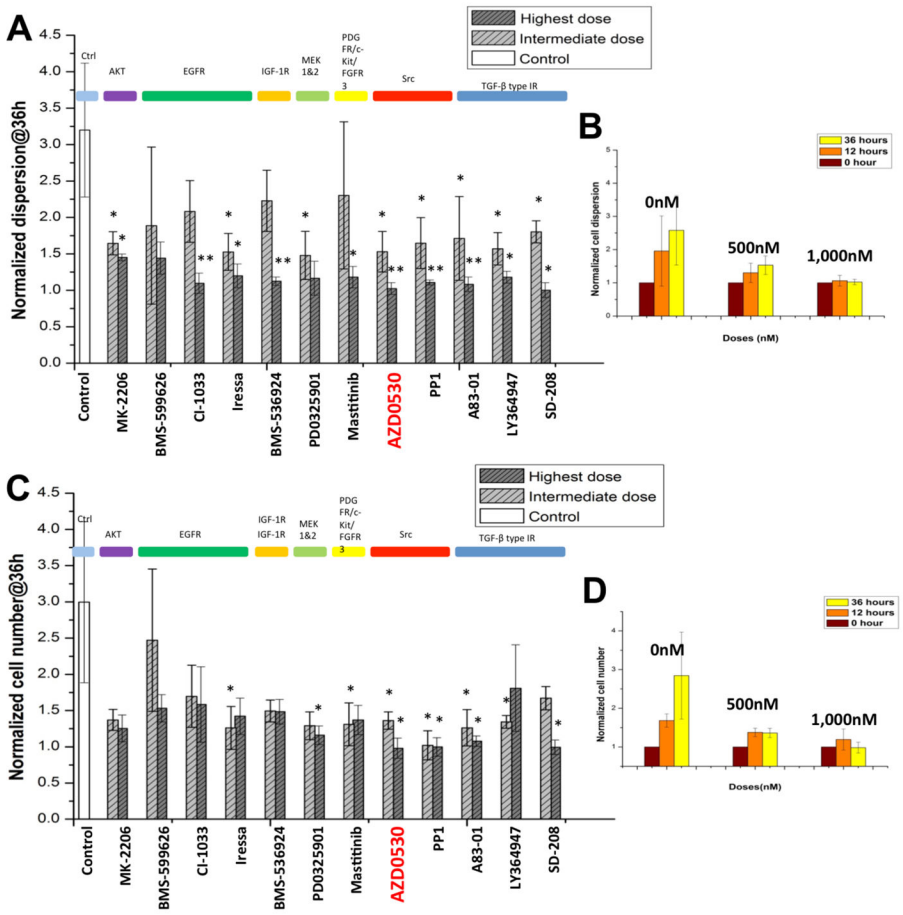

Fig. 5.

Analysis of cell dispersion and proliferation in the presence or absence of drug treatment. A. Normalized dispersion for twelve drugs. B. Representative normalized dispersion measured over time for three concentrations of AZD 0530. C. Normalized proliferation for twelve drugs. D. Representative normalized proliferation measured over time for three concentrations of AZD 0530. The values for the effective dose for full inhibition are given in Table 1.

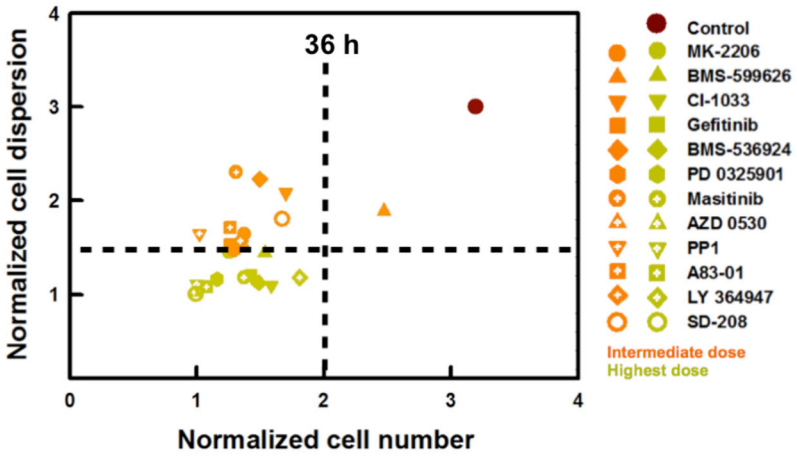

Fig. 6.

Normalized cell dispersion and corresponding cell number at 36 h. Four quadrants were defined to characterize the dose response for each drug. The \upper right quadrant indicates cases with high rates of proliferation and dispersion, where we find the control conditions. Most drug-treated data lie in the lower left quadrant with low proliferation and low dispersion activity. Therefore, it appears that for the conditions tested, drugs reduced cell dispersion and cell proliferation simultaneously.

Table 1

Targeted inhibitors and doses used in this study. Effective dose represents the dose required for full inhibition of dispersion in 3D after 36 h incubation

Targeted inhibitors used in this study. Twelve drugs were selected targeting inhibition of EGFR, IGFR, PDGFR and TGF-βRI/ALK5-dependtent activation, as well as through intracellular kinases such as Src, MEK and AKT. IC50 values of 2D dispersion assay for twelve drugs were determined. In addition, dose required for full inhibition in 36 h incubation in 3D microfluidic co-culture. The “effective dose” was determined by the lowest tested concentration deemed sufficient to prevent dispersion.

Name	Target	Development stage	Inventor/sponsor	2D dispersion assay	3D dispersion assay
				IC50(nM)	Effective dose(nM)
MK-2206	AKT	Phase 1, 2	Merck	>5,000	300
BMS-599626	EGFR	Phase 1	Bristol-Myers Squibb	3,500	200
CI-1033	EGFR	Phase 1, 2	Pfizer	5,200	300
Gefitinib	EGFR	FDA approved	AstraZeneca	3,000	500
BMS-536924	IGF-1R, IR	Research	Bristol-Myers Squibb	-	1,000
PD 0325901	MEK1, MEK2	Phase 1, 2	Pfizer	>5,000	25
Masitinib	PDGFR, c-Kit, FGFR3	Phase 1, 2, 3	AB Science	1,200	1,500
AZD 0530	SRC, ABL	Phase 1, 2	AstraZeneca	2,100	1,000
PP1	SRC	Research	Pfizer	>5,000	5
A83-01	TGF-β type IR	Research	Kyoto Pharmaceutical University	430	7.5
LY 364947	TGF-β type IR	Research	Eli Lilly	>5,000	1,000
SD-208	TGF-β type IR	Research	Scios	>5,000	500